From Highly Efficient Impurity-Free CNT Synthesis to DWNT forests, CNTsolids and Super-Capacitors

Kenji Hata
Research Center for Advanced Carbon Materials, National Institute of Advanced Industrial Science and Technology (AIST), Tsukuba, 305-8565, Japan

ABSTRACT

We demonstrate an extremely efficient chemical vapour deposition synthesis of single-walled carbon nanotubes where the activity and lifetime of the catalysts are enhanced by controlling the ambient of the CVD furnace, a growth mode we call "Super Growth" [1]. The enhanced catalytic activity of super growth results in massive growth of super-dense and vertically-aligned single-walled nanotubes forests with heights up to 2.5 millimeters. In addition, these SWNT forests were easily separated from the catalysts, producing the most pure SWNT material (over 99.98%) ever made, through an all-dry process without any purification. Moreover, patterned highly organized intrinsic single-walled nanotube structures were successfully fabricated. Super Growth simultaneously addresses many critical problems such as scalability, purity, and cost, and opens up innumerable opportunities ranging from fundamental research to real applications.
Keywords: Carbon nanotube, single-walled carbon nanotube, chemical vapor deposition, synthesis

1. INTRODUCTION

Single walled carbon nanotube (SWNT) is a key aspect in the emerging paradigm of nanotechnology; however, large-scale, real products have not yet been realized because of the problems surrounding the difficulties in synthesizing SWNTs, such as limited availability, low purity, and extremely high cost. Current synthesis methods suffer from large concentrations of impurities and thus require purification of the as-grown product that results in the degradation of the nanotubes and an increase in the cost. Furthermore, dispersion of SWNTs in solutions and reconstructing them into desired organized structures have proven to be extremely difficult. Here we report a rational yet simple and general synthetic approach that concurrently addresses these problems where the activity and lifetime of the catalysts are dramatically enhanced by the addition of a controlled amount of water vapor in the growth ambient (henceforth denoted as "Super Growth chemical vapor deposition (CVD)") [1]. With the assistance of water, super-highly dense, vertical-standing, and aligned SWNTs forests with heights up to 4.0mm were synthesized, representing a 100 times increase in efficiency over previous records. In addition, these SWNT forests were easily separated from the catalysts, producing the most pure SWNT material (over 99.98%) ever made, amazingly through an all-dry process without any purification. Moreover, highly organized intrinsic SWNT structures were successfully fabricated. These results represent a major breakthrough in highly pure and highly efficient SWNT synthesis and consequently unlock a multitude of new unexplored opportunities in such areas as biology, magnetic and optical properties, and solution-based chemistry.

2. EXPERIMENTAL

Our synthesis approach was motivated to find a weak oxidizer to selectively remove amorphous carbon but to not damage the nanotubes at the growth temperature because it is understood that coating of the catalytic particles by amorphous carbon during CVD reduces their activity and lifetime. This is the most serious obstacle in current SWNT CVD synthesis. We found that water acts dramatically in promoting and protecting catalytic activity. SWNTs were grown by ethylene CVD using Ar or He with H_2 that contained a small and controlled amount of water vapor. Balancing the relative levels of ethylene and water was crucial to maximize catalytic lifetime.

Water-assisted growth was successfully carried out on various catalysts that provide SWNTs (Fe nanoparticles[2] by $FeCl_3$, sputtered metal thin films (Fe, Al/Fe, Al_2O_3/Fe, Al_2O_3/Co)) on Si wafers, quartz, and metal foils, demonstrating the high generality of our approach. SWNTs were synthesized using Ar or He with H_2 as a carrier gas (total flow 1 m^3 STP per minute) at 1 atm with controlled amount of water vapor (concentration 100 ppm to 500 ppm). Various catalysts

known to provide SWNTs (Fe nanoparticles2 by $FeCl_3$, sputtered metal films (Fe (1 nm), Al(10 nm)/Fe(1 nm), Al_2O_3 (10 nm)/Fe(1 nm), to Al_2O_3 (10 nm)/Co(1nm)) were deposited on Si wafers or quartz or metal foils and placed in a quartz tube furnace. Growth was carried out at 750°C with ethylene (20-75 cm^3 STP per minutes) for 10 min as the typical growth time. To make SWNT solids, collapse of as-grown forests was typically performed using a highly diluted ethyl alcohol solution. Depending on the desired purpose, forests were removed from the catalytic surfaces and placed into a small beaker containing the alcohol solution where the collapse process began. As the liquid enters the inter-tube regions, noticeable decrease in the physical dimensions occurs, after which it sinks. At that time, they are removed from the solution and allowed to dry on a clean silicon surface where the final stage of the collapse occurs.

3. RESULTS AND DISCUSSION

3.1 Synthesis of vertically aligned SWNT forests

Extremely high water-stimulated catalytic activity results in massive growth of super-dense and vertically-aligned SWNTs forests with height on the millimeter-scale in a 10 minute growth time. Figure 1a shows a 2.5 mm height SWNT forest that was presented in 2004 [1]. In sharp contrast to standard ethylene CVD growth, where the catalysts are only active for about a minute, some height increase of the forests has been observed after 30 min for water-assisted growth, clearly demonstrating the role of water as a protecting agent of the catalysts. The SWNT/catalyst weight ratio exceeds 50,000%, more than 100 times higher than other processes, illuminating the remarkable efficiency of water-assisted nanotube synthesis. A close examination (Fig. 1b) at the ledge of the SWNT forest illustrates that the nanotubes are densely packed and well aligned vertically from the substrate. High-resolution transmission electron microscopy (TEM) studies (Fig. 1c) show that the nanotubes are clean SWNTs free from amorphous carbon and metal particles. Low-resolution TEM studies (Fig. 1d) of the as-grown forest reveal the presence of only thin nanotubes and the absence of metallic particles and supporting materials that usually comprise a major constituent of as-grown material. Raman spectra showed clear radial breathing mode peaks that correspond well with the size of the SWNTs measured by TEM. Thermo-gravimetric analysis (TGA) on pure SWNT material using N_2 gas with water shows that SWNT combustion by water starts at about 950°C, indicating that the water does not oxidize and damage the nanotubes at the growth temperature.

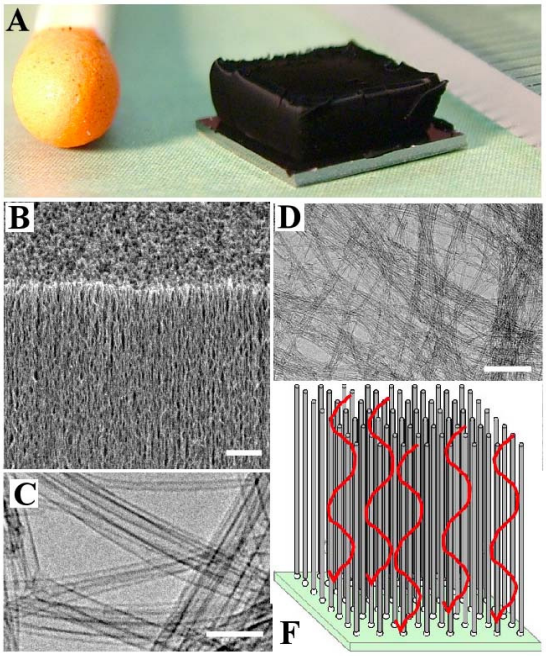

Fig. 1. A Picture of an single-walled carbon nanotube forest (SWNT). B Scanning electron microscopy (SEM) image of the SWNT forest ledge. C High resolution tramission electron microscopy (TEM) image of SNWTs. D A large area TEM image. E Schematic of the structure of the forest. The catalysts are fixed on the substrate. SWNTs grow out from the catalysts and stand vertically. Carbon sources have to diffuse through the nanotubes to reach the catalyst.

The catalyst activity, mass density and tube density of SWNT forests were estimated by a statistical and macroscopic analytical approach [2]. For a typical SWNT forest, the SWNT area density is 5.2 x10^{11} tubes/cm^2, the mass density of the forest is 0.037 g/cm^3, the average SWNT size is 3.0 nm, and the SWNT area density is 5.2 x10^{11} tubes/cm^2. The catalyst activity was estimated to be 84% (±6 %), which is an very high value when compared to the few percent activity in normal CVD. These numbers mean that on average there exists one 3 nm diameter SWNT in a substrate area of 190 nm^2 and that the average distance between tubes is 14 nm. Consequently, The SWNT forest is a very sparse material where SWNTs represent only 3.6% of the total volume the SWNTs occupy 3.6% of the total volume, thus meaning that more that 96% is empty space, as displayed in a schematic (Fig. 1(e)) of the forest assuming complete uniformity .We believe the sparseness of the forest is essential for growing SWNT forests by CVD where the catalysts remain on the substrate during growth (root growth) as is the case for super-growth. We suspect that excessively high densities inhibit carbon diffusion to the catalysts (diffusion limited); whereas, for insufficiently high densities, the SWNTs would fail to grow vertically and form a mat and likely quickly suffocate the catalysts as observed in normal CVD. With this sparseness, vast amounts of SWNTs can be grown on a substrate while not restricting the delivery of the carbon feedstock.

3.2 Catalyst free as-grown SWNTs

The SWNT forest structure can be easily removed from the substrate using, for example, a razor blade. After removal, the substrate is still catalytically active to grow SWNT forests again, which clearly indicates a root-growth mode and the presence of the catalysts on the substrate. The high SWNT/catalyst weight ratio, the clean TEM images in Figs. 1 and Figs. 2, and the easy removal of the forests suggest that the as-grown SWNT material is highly pure. Low-resolution transmission electron microscopy (TEM) studies (Fig. 2) of the as-grown forest reveal the presence of only thin nanotubes and the absence of metallic particles and supporting materials that usually comprise a major constituent of as-grown material (inset of Fig. 2). High-resolution TEM studies (Fig. 1c) show that the nanotubes are clean SWNTs free from amorphous carbon and metal particles.

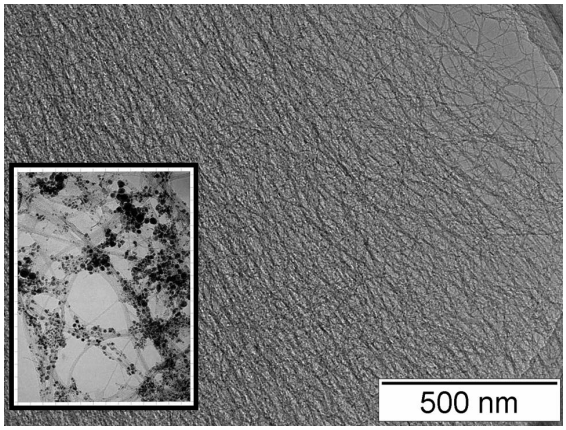

Fig. 2. A Transmission electron microscopy (TEM) image showing the as-grown SWNTs of the forest. Inset: A TEM image of the as-grown SWNTs synthesized from normal chemical vapor deposition (CVD).

To investigate this important point and to address other issues, thermo-gravimetric analysis (TGA) was implemented on 10 mg of the as-grown material. No measurable residue remained after heating above 750°C, indicative of carbon purity above 99%. The combustion range of the SWNTs was 550°-750° C with the peak weight reduction occurring at 700° C, a result very similar to that of purified, high-quality SWNTs synthesized by laser oven. Quantitative elemental analysis with X-ray fluorescence spectrometry detected 0.013% Fe as the only impurity, meaning a carbon purity over 99.98%, i.e. the most pure SWNT material ever made. We believe that this extremely pure SWNT material opens up countless new opportunities. For example, it should serve as an ideal standard material for biological research due to the lack of possible toxic metal particles and amorphous carbon, and thus it should settle the controversial issue regarding the

toxicity of SWNTs. Furthermore, pure SWNTs should allow for the investigation of the intrinsic magnetic properties of SWNTs, a field that has been widely unexplored mainly due to magnetic metal impurities.

3.3 Organized and Patterned SWNT forests

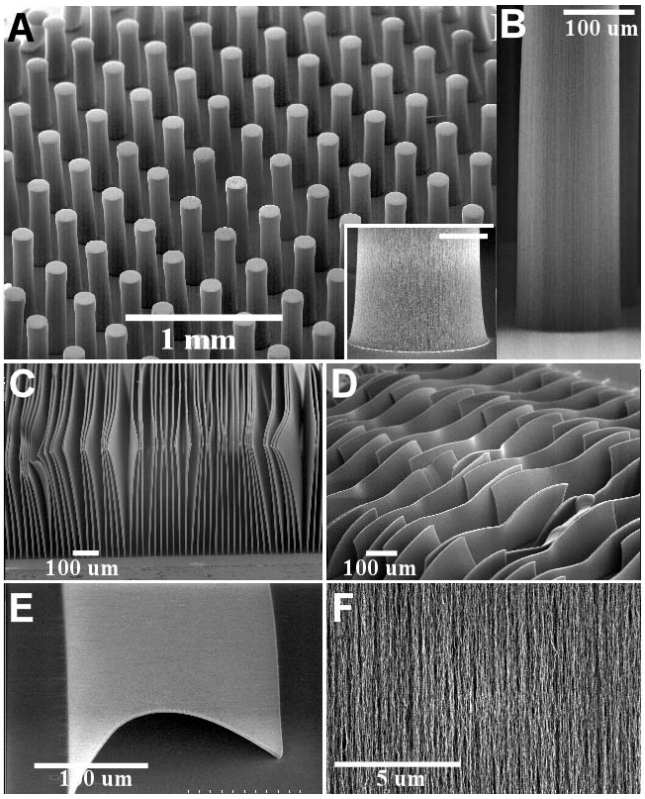

Fig. 3. A set of SEM images showing patterned SWNT forests. A SEM image of SWNT cylindrical pillars with 150-um radius, 250-um pitch, and -1-mm height. Inset, SEM image of a root of a pillar. Scale bar, 50 um. B side view of a pillar. C and D SWM images of SWNT sheets. E SWM image of an isolated SWNT sheet. F SEM image of the sheet face..

Realization of large-scale organized SWNT structures of desired shape and form is important for obtaining scaled-up functional devices. For MWNTs successful fabrication of organized structures has been demonstrated, though it remains to be seen if similar structures could be made from SWNTs that are much smaller in size and thus naturally much more difficult to self-align vertically. Significantly, with the assistance of water, SWNTs grow easily from lithographically patterned catalyst islands into well-defined vertical-standing organized structures, as demonstrated by the large-scale arrays of macroscopic cylindrical pillars (Fig. 3a) with 150 μm radius, 250 μm pitch and a height close to 1 mm. A close examination (Fig. 3b) shows that the pillars are vertically standing straight from the substrate. Importantly, the cross section of the SWNT structure corresponds well with the patterned catalyst (inset of Fig. 3a), and thus it is possible to fabricate arbitrary shapes of organized SWNT structures where the base is lithographically defined and the height is controlled by the growth time. To further explore this unique opportunity, we templated rows of catalytic stripe patterns, and succeeded in growing pseudo two-dimensional organized SWNT structures (Figs. 3c and d) that resemble sheets. A close investigation of a sheet face (Fig. 3f) reveals that the SWNTs are well aligned with high uniformity. Interestingly, some of these sheets are curved like pages in a book, demonstrating their flexibility. This important aspect is highlighted in Fig. 3e where an isolated thin SWNT sheet of thickness of 5 μm was fabricated. While this sheet formed a well organized structure, its flexibility allowed it to bow and touch the surface, a point that suggests these thin sheets could be arbitrary laid down, for example, by using mechanical forces, or gas flows or electric fields. When a patterned array of sheets is laid down on the substrate to form large-scale aligned SWNT films, they might serve as a unique functional SWNT material that would find applications, such as an optical polarizers and anisotropic conductive material.

3.4 Kinetics of Super-Growth

Knowledge of the kinetics is critically important to understand the mechanism of the super-growth CVD. We have addressed this issue by formulating a numerical growth model that describes the time-evolution of the super-growth [3]. This growth model served as the key point to quantitatively analyze the kinetics of the super-growth and to gain insight into the effect of water. We found it possible to evaluate the SWNT yield for a given growth condition simply by measuring the height of the SWNT forest. The time-evolution of the forests heights (yield) at a fixed growth condition (Fig. 4) showed that the growth rate was highest at the onset of growth, gradually decreased over the subsequent 20 minutes, and finally terminated with a height of 970 μm.

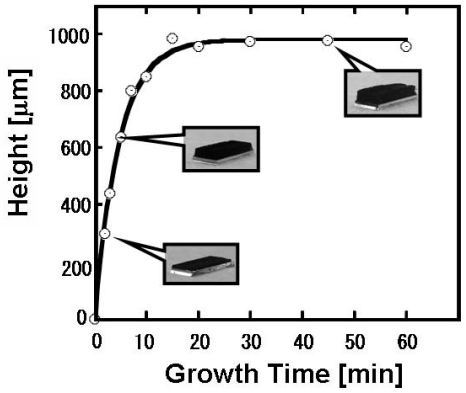

Fig. 4. Time evolution of SWNT forest growth. Plot of the SWNT forest height as a function of the growth time

We modeled this time-evolution by assuming that the catalysts lose their activity in a similar fashion to radioactive decay. Assumptions we made were: (1) the catalysts showed identical activity, (2) the increase in yield of SWNTs (and thus the height of forests) was directly proportional to the number of active catalysts; and (3), the number of catalysts that decay was proportional to the number of active catalysts. With these assumptions the time evolution of the height of the forest growth rate could be expressed, as $H(t) = \beta\tau_o\left(1 - e^{-t/\tau_o}\right)$.

It is very important to note that an important physical meaning can be assigned to the two fitting parameters: β is the initial growth rate (IGR) and τ_o is the characteristic catalyst lifetime. Fitting our growth-equation to the experimental time-evolution data yielded excellent agreement ($R^2 = 0.9940$) as demonstrated by the solid line in Figure 1, supporting the soundness of our modeling. The fitting parameters for this specific growth condition were: IGR (β) of 207 μm/min and lifetime (τ_o) of 4.74 minutes, respectively. Interestingly, according to the growth-equation, the product of the two fitting parameters, $\beta\bullet\tau_o$,gives the theoretical maximum height, H_{max},, and for this specific growth condition H_{max} is calculated to be 980 μm which matches very well with the experimentally obtained maximum height 970 μm.

This time-evolution analysis can be carried out on a variety of growth conditions to study the kinetics of the super-growth. A family of time-evolution data of the super-growth fitted with the growth-equation taken at different ethylene flow rates at a fixed water level. The family of growth-equation curves exhibits a particularly complex behavior: as the ethylene level increases, not only does the maximum height raise then fall, but also many crossings among curves occur. The apparent complexity of the family curves hinders our ability to gain further insight into the kinetics of the super-growth; however, we found that the analysis of the fitting parameters renders this complexity into a readily explainable phenomenon. From each growth-equation curve, the initial growth rate β and the characteristic catalyst lifetime τ_o was calculated and plotted as a function of the ethylene flow rate (Figure 5). Overall, the lifetime and IGR followed divergent trends, ie the IGR monotonically increases while the lifetime decreases with the ethylene level. The existence of these crossings among growth-equation curves is a direct result of this divergent trend: slower initial growth with long lifetimes achieves higher maximum heights than rapid initial growth but with short lifetimes. Furthermore, despite this divergent trend, the theoretical maximum height (Figure 2(b) as a histogram), being the product of the two fitting parameters, $\beta\bullet\tau_o$, exhibits a peak representing the optimum ethylene flow rate for this water level. The divergent trends

are easily explainable: (1) IGR monotonically increases with ethylene because the carbon source for SWNT growth increases, (2) lifetime decreases since the catalysts are poisoned faster by rapid accumulation of amorphous carbon coating, a factor known to kill catalyst activity. A close examination of the trend at low ethylene levels shows that the lifetime increases until 100 sccm, and IGR shows a sharp increase up to about 50 sccm. This significant different behavior than the overall trend results from the water-assisted increased growth efficiency, and reflects the ethylene level approaching the optimum growth condition for this water level.

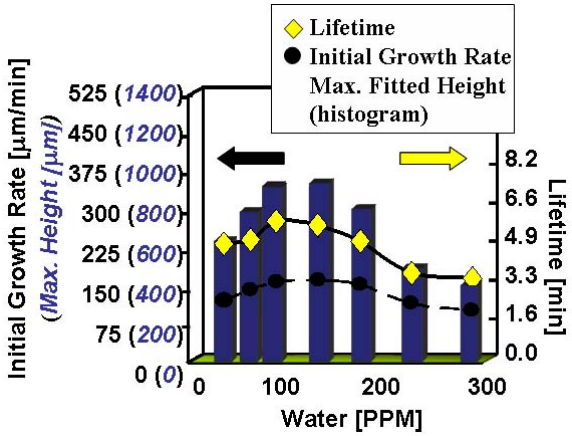

Fig. 5. Overlaid plots of the lifetime, initial growth rate, and maximum height (histogram) as derived from each growth curve

Further analysis was carried out by the two-dimensional mapping of the dependence of the lifetime, initial growth rate, and theoretical maximum height on water and ethylene. The map for the theoretical maximum height proved to be quite complex and neither provided further insight into the growth kinetics nor served as a useful guide to identify the optimum growth condition. However, we discovered that we could deepen our understanding by rearranging the data of Figure 4 into a plot of the maximum height as a function of the water/ethylene ratio (Fig. 6). Interestingly, a clear trend emerged by this rearrangement, despite spanning a wide range of growth conditions (ethylene 10-300 sccm; water 50-290 ppm). The maximum height initially increased with the water/ethylene ratio, peaked at a value of about 1/1000, then decreased with further increase of the water/ethylene ratio. The water-assisted enhanced growth efficiency is reflected in the initial increase of the maximum height, and the peak represents the optimum growth conditions of the super-growth for this growth temperature and catalyst. The existence of such a peak demonstrates that there exists a scaling relation between ethylene and water and that the balance of the ethylene and water is the most critical factor for the super-growth. By this we mean that the same maximum height can be achieved by both a slow growth with a long lifetime and a fast growth with a short lifetime given that the water/ethylene ratio is the same. Furthermore, the existence of this scaling law suggests that the catalysts consume a specific number of ethylene and water molecules before they die, and this specific number is determined by the water/ethylene ratio. Moreover, it implies that each growth event in which a carbon atom is supplied from the gas phase, incorporated into a catalyst, and solidified as a SWNT can be considered as a Markov process, i.e., growth events are independent. This implies that the rate limiting process of the SWNT growth in this growth parameters window is the supply of carbon to catalysts from the gas phase.

3.5 Growth of double-walled carbon nanotubes forests from engineered iron catalysts

Double-walled carbon nanotubes (DWNTs) are a unique form of carbon nanotubes (CNTs) as being composed of two coaxial single-walled carbon nanotubes (SWNT); therefore, they benefit from a synergetic blend of both SWNT and multi-walled carbon nanotube (MWNT) characteristics and thusly exhibit the electrical and thermal stability of MWNTs and yet the flexibility of SWNTs. The most prominently pursued application of DWNTs is electron emitters because DWNT emitters low threshold voltage as that of SWNTs and MWNTs-like durability. Synthesis of catalyst-free DWNT forests with millimeter-scale height was possible by super-growth CVD by using catalyst nanoparticles tailored to achieve maximum DWNT selectivity [4]. Catalyst engineering was the key point for selective DWNT synthesis and was achieved by determining the optimum mean tube diameter for selective DWNT synthesis and by growing CNTs with

this optimum mean diameter by precisely controlling the thickness of the Fe catalyst film. from catalyst nanoparticles tailored to achieve maximum DWNT selectivity. To understand and control CNT synthesis, we first studied the relationship between the tube type and diameter by constructing a phase diagram (Fig. 6a) of the relative populations of SWNTs, DWNTs, MWNTs vs. the tube diameter from the analysis of 1432 CNTs by TEM. The phase diagram evidences that DWNTs occupy the majority of the nanotube population within a distinct diameter range, 3.0 to 4.5 nm, sandwiched between the SWNT and MWNT regions. The existence of this distinct DWNT region affords selective DWNT growth via tuning the tube diameter into this DWNT region. The DWNT region predicts that the maximum DWNT selectivity occurs when the mean CNT diameter is around 3.75 nm. In addition, we found that the mean CNT diameter can be precisely tuned by controlling the thickness of the Fe thin film. The mean CNT diameter was found to increase approximately linearly with the thickness of Fe thin film thickness (Figure 6b). This important finding made it possible for us to accurately control the mean CNT diameter into the DWNT region.The maximum DWNT selectivity achieved with our approach was 85% as shown in the DWNT (and SWNT, MWNT) diameter and population distribution of this sample in Figure 2c. This DWNT selectivity is one of the highest reported, and is worth noting that it was achieved on an as-grown sample without any additional processes implemented to improve selectivity. The maximum DWNT selectivity was achieved when the Fe thin film thickness was 1.7 nm from which DWNTs with an average diameter of 3.7 nm were synthesized. These results correspond well with our estimation, highlighting the controllability of our approach.Water-assisted CVD was implemented to demonstrate highly-efficient DWNT syntheses from these engineered catalysts. Similar to the case of SWNTs, water-assisted CVD resulted into massive growth of DWNTs that self-organize into vertically-aligned DWNT forests with millimeter-scale height. TEM images show only clean nanotubes which are mainly DWNTs. TGA of the as-grown material showed no measurable residue, indicating very high purity. Furthermore, elemental analysis with x-ray fluorescence spectrometry detected the presence of only 0.053 wt% Fe as the sole impurity, meaning a carbon purity over 99.95 wt%. These results demonstrate that it is possible to grow DWNT forest with the same quality yield, and purity with super-growth CVD

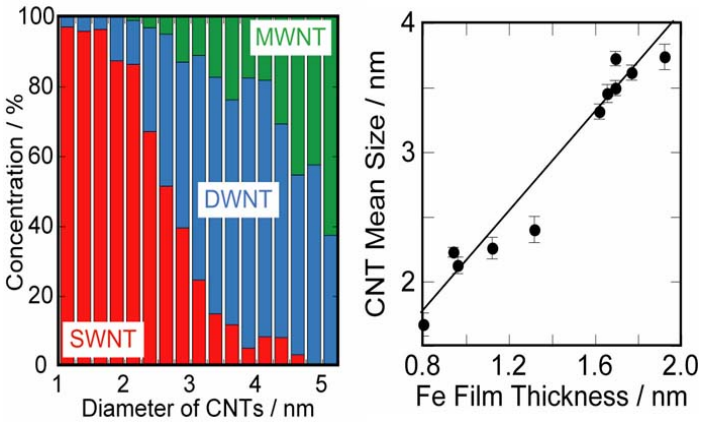

Fig. 6. Trends in CNT type and diameter. (a) Phase diagram of the relative concentration of SWNTs (red), double-walled carbon nanotubes (DWNTs) (blue) and multi-walled carbon nanotubes (green) as a function of the CNT diameter. (b) Plot of CNT mean diameter as a function of Fe film thickness.

3.6 Growth of SWNT forests on metal foils

Generally, SWNT syntheses have been implemented on insulating substrates, such as Si wafers or quartz. In many cases, growths on conducting substrates is desired but have resulted in the formation of multi-walled carbon nanotubes (MWNTs) or graphite films. The difficulty to efficiently grow SWNTs on conducting films restricts device architectures and fabrication processes for nano-electronic devices. We found that foils made of Ni-based alloys with Cr or Fe were excellent for SWNTs (DWNTs) synthesis [5]. DWNTs grown on these substrates showed homogeneous field emission throughout the entire cathode grid, thus providing evidence of electric contact between the DWNTs and the metal foils. These results open up an economical route for the mass production of SWNT (DWNT) forests and also enable the straightforward integration of SWNTs (DWNTs) into nano-electronic devices, such as field emission displays.

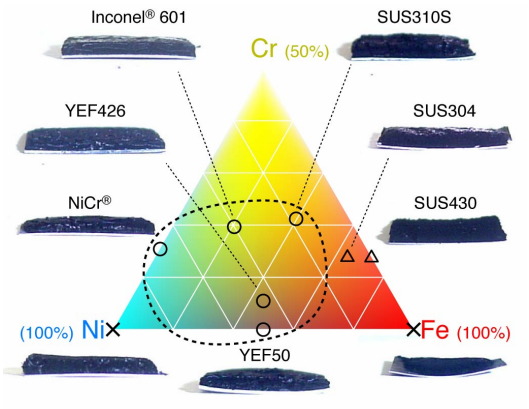

Fig. 7. Trends in CNT type and diameter. (a) Phase diagram of the relative concentration of SWNTs (red), double-walled carbon nanotubes (DWNTs) (blue) and multi-walled carbon nanotubes (green) as a function of the CNT diameter. (b) Plot of CNT mean diameter as a function of Fe film thickness.

Importantly, we did find that Ni-based alloys with Cr or Fe possessed both high durability to the CVD ambient and the ability to support highly efficient SWNT (DWNT) synthesis. Successful syntheses of SWNT forests were achieved on various alloys spanning many standard metals, such as, Inconel® 601, YEF 426, NiCr®, YEF 50, SUS 310S, covering a wide range of Ni-Fe-Cr compositions (Figs. 6). Transmission electron microscopy (TEM) analysis showed that the growth product was mainly SWNTs with selectivity of 95%; a result similar to the level achieved on Si wafers. Furthermore, the efficiencies of the water-assisted growths on these foils were high, almost approaching the level of Si wafers. The G-band/D-band ratios of the Raman spectra of the forests revealed that the SWNTs grown on Ni-based foils and Si wafers were of the same quality level. These experimental results show that Ni-based alloys with Fe/Cr are excellent substrates for SWNT synthesis. In contrast, detailed TEM analysis revealed that CNTs grown on Ni, Fe, and two Fe-Cr alloys (SUS 430, SUS 304), consisted not only of SWNTs but also of MWNTs.

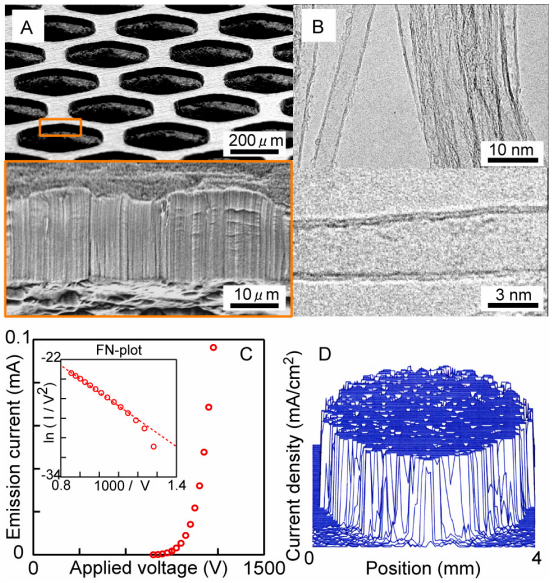

Fig. 8. Double/YEF 426 as an electron field emitter. (a) Scanning Tunneling microscopy images of a DWNT forest directly grown on a YEF 426 grid. (B) TEM images of DWNTs. (C) Emission current versus applied voltage profile. (D) Emission distribution profile of an electron emitter at a display range of 0.001-1.00 mA/cm^2

To demonstrate versatility of CNT forests as electrodes and direct electric contact of CNT forests with the foils, field electron emission from a CNTs/foil cathode to anode was measured. To this end, we grew a short DWNT forest on a 1 cm diameter YEF 426 metal cathode (Fig. 8a). DWNTs were synthesized here because of their superior field emission properties. TEM images (Fig. 8b) confirmed that the majority of CNTs synthesized were DWNTs. The ability to control the selectivity of SWNTs and DWNTs highlights the controllability and reliability of Ni-based alloys for CNT synthesis. The emission current exponentially increased with increasing electric field (Fig. 8c), following the Fowler-Nordheim equation. The spatial mapping of the emission current at the range of 0.00-1.00 mA/cm^2 showed an excellent homogeneity (Fig. 8D), a important point for the practical application toward field emissions displays. Homogeneous emission from the DWNT electrodes is direct evidence of good electrical contact between DWNTs and the grid substrate. Metal foils are much more economical and scalable than Si wafers or quartz substrates. Therefore, we believe that this approach opens up an economical route towards mass production of SWNT (DWNT) forests, and will facilitate flexible design of device architectures and fabrication processes for CNT-devices.

3.7 SWNT solid - Shape-engineerable and high-densely packed single-walled carbon nanotubes

CNT possesses excellent electrical, thermal, and mechanical properties; however macroscopic forms of CNTs lose the intrinsic properties of individual CNTs. To address to this matter, various CNT forms have been demonstrated ranging from fibers, yarns, mats, vertically-aligned CNTs (forests), powders, pellets, foams, and sheets. Yet, it is difficult to simultaneously retain the fundamental SWNTs properties, such as high surface area and electrical conductivity on a macroscopic scale and have versatility in creating different shapes. This stems from the fabrication processes, which can either damage the tubes or is unable to control the configuration of the tubes within the forms, or both. For example, pellets are brittle, forests are fragile, and fibers, yarns and sheets are limited to a single shape. A new macroscopic bulk form of CNT material which we call the "SWNT solid" is presented in which aligned SWNTs are densely packed while retaining the intrinsic properties of SWNTs, such as high surface area, flexibility, and electrical conductivity [6]. Importantly, the shape is engineerable by controlling the fabrication process, which is beneficial for applications spanning from 100% binder-free SWNT electrodes for capacitors to flexible heaters.

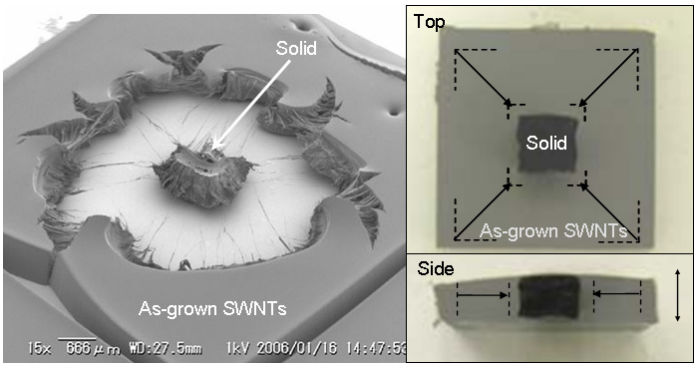

Fig. 9. Liquid induced collapse. a, Scanning electron microscope (SEM) image of SWNT forest structural collapse from a single drop of liquid. b, Overlaid pictures illustrating the decrease in lateral dimensions before (grey) and after (black) collapse. The double-ended arrow indicates tube alignment direction.

Our approach to fabricate high density SWNT bulk solid exploits a liquid-induced collapse of SWNT forests (Fig. 9). When liquids are introduced into the sparse as-grown SWNT forest and dried, the surface tension of liquids, and strong van der Waals interaction effectively "zippers," the SWNTs together to near ideal graphitic spacing. This packing occurs in two steps: liquid immersion and evaporation. In the first step, the tubes are drawn together through liquid capillary forces and the forest decreases ~20 % in lateral dimension Upon liquid evaporation, van der Waals forces adhere the tubes near to ideal packing transforming, a forest into a small and rigid single body as demonstrated in Fig. 9a, where a 1 x 1 cm as-grown SWNT forest was contacted by a drop of water in the middle and dried. Liquid-induced collapse shows a 4.5-fold decrease in the two lateral dimensions while no detectable change in the height, producing a ~20-fold increase in mass density (Fig. 9b). This indicates that alignment of the as-grown forest is critical in triggering efficient liquid induced collapse, an understandable point because the aligned nature provides an ideal condition for optimum van der

Waals overlap. Unlike as in Fig. 9a, the as-grown forest material was removed from the substrate and completely immersed into a liquid to provide uniform collapse. The zippering action proceeds without damaging the tubes. the density was roughly estimated to be 0.55 g/cm^3, a number comparable to that of activated carbon. The initial 97% empty space in forests reduced to ~50% and the inter-tube and inner-tube volumes becomes equivalent. The Vickers hardness of the SWNT solid increases over 70-fold to 7-10 which is comparable with that of highly oriented pyrolytic graphite (HOPG). The above characterization highlights the solidness and unity of the liquid induced collapsed material, and thus we call this form a SWNT "solid." Significantly, the SWNT solid possesses a high surface area almost identical to the as-grown forest despite the highly dense packing of SWNTs, meaning a considerable increase in the volumetric adsorption density, an indicator of surface area per unit volume. The estimated Brunauer-Emmett-Teller (BET) surface area for the solid, as determined from nitrogen adsorption isotherms, was 1000 m^2/g, being similar to that of as-grown SWNTs. These surface area values are much higher than that measured for closed HiPco samples (520 m^2/g). The volumetric adsorption density jumps 20-fold compared to the as-grown forest. Furthermore, SWNT solids have a comparable or superior surface area and volumetric adsorption density than SBA-15, a standard mesoporous silica material.

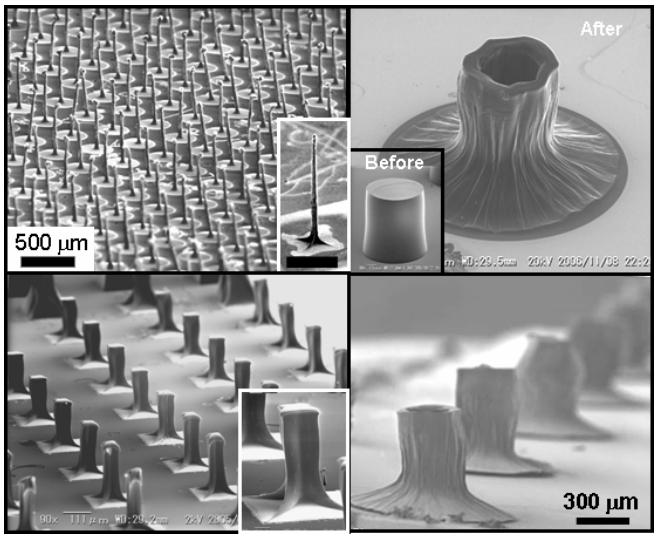

Fig. 10. Engineerable shape. a, SEM image of an array of lithographically designed solid needles. Inset, magnified individual needle. Scale bar, 60 μm.b, SEM image of a "micro-volcano.". Inset, "micro-volcano" prior to collapse. c, and d, Arrays of shaped solid structures.

The SWNT solid concept can be extended to create a variety of unique solid structures from as-grown forest material with diverse shapes by controlling parameters that influence the collapse process, such as forest aspect ratio, initial liquid contact point, and substrate-forest interaction. For example, lithographically defined as-grown SWNT circular pillars with high aspect ratio collapsed from the tip creates well-defined and patterned SWNT solid needles with high aspect ratio (Figs. 10). In high contrast, low aspect ratio SWNT circular pillars with strong substrate interaction collapsed from the surface edge results in a vastly different structure resembling a "micro-volcano". The peripheral collapse draws nanotubes radially outward from within the pillars, thus creating a cavity. Another approach to extend our ability to engineer the shape of the solid is to employ moderate external forces, such as very light pressure, to direct the direction of the collapse. For example, applying light pressure in one lateral direction suppresses collapse in one lateral dimension and creates a bar (Fig. 11). Similar application of light pressure at a shearing angle to the alignment induces a vertical collapse, without any collapse in both lateral dimensions, results in a solid sheet. Because the SWNTs are directed to lay like a field of corn stocks flattened by a tractor, the solid sheets maintain a comparable degree of alignment of the forest, and the direction of alignment is controllable by changing the direction of pressure. This approach is easily extendable to fabricate strongly adhered solid sheets on desired flat substrates without the use of bonding agents by simply transferring the forest onto a target substrate and implementing the collapse process, exampled by a 1 mm tall, 1 x 1 cm forest collapsed into a 1 x 1 cm, optically flat solid sheet with a height less than 100 μm strongly adhered on a copper contact,

a form useful for multiple uses. The ability to engineer the shapes of solids is beneficial for a multitude of applications requiring high surface area, high density, aligned, conducting, and flexible or rigid CNT material. The SWNT solids represent substantial progress towards producing macroscopic scale high density SWNT material engineered in both shape and structure opening diverse functionality that is advantageous for numerous applications, such as energy storage. Our approach is unique from other existing processes to make CNT forms, e.g., those that use dispersion solutions, because nanotube are not harmed and thus the properties of SWNTs are retained on the macroscopic scale material. We believe that our approach can be extended further to make new and sophisticated CNT forms by using more complex SWNT forests or introducing different materials into the system.

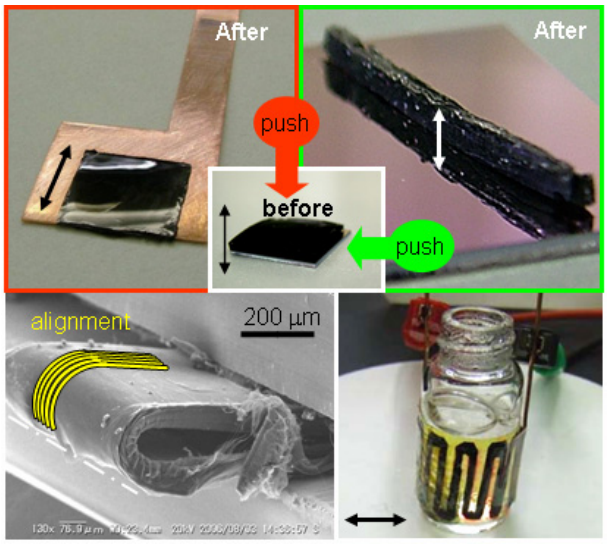

Fig. 11. a, Flexible SWNT solid engineered into a flattened sheet adhered to a copper sheet.. Inset, Photograph of the as-grown forest. b, SWNT solid engineered into a rigid "bar.". c, SEM image of the SWNT sheet with radius of curvature ca. 35 mm illustrating the good flexibility when CNT alignment is perpendicular to the curvature. Yellow bars illustrate the SWNT alignment direction.d, Flexible heater. Photograph of a SWNT solid-based flexible heater boiling water. The double-ended arrow indicates tube alignment direction.

4. CONCLUSION

Super-growth CVD possesses the simplicity and generality to be applicable to other existing synthesis methods developed for the mass production of SWNTs, such as rotary-kiln, floating catalyst, and fluidized bed. More directly, mass production might be realized by substrates with increased surface area, for example on waffled foils, addressing simultaneously many critical problems such as scalability, purity, and cost, and thus our approach represents a significant advance towards a realization of large-scale SWNT products. When combined with the ability to control the SWNTs diameter by tailoring the catalysts size and the recently reported selective growth of semiconductive SWNTs by plasma assistance, the approach provided herein should enable unprecedented mass-production of SWNTs with controlled properties that possess enough purity for immediate use in various applications ranging from biology, magnetic and optical properties, and solution-based chemistry. These SWNTs could be grown into scaled-up macroscopic organized structures with defined shape, be it a three-dimensional complex structure or a two-dimensional flexible sheet, that could be developed into systems including field emitter arrays for flat panel displays and optical components, such as polarizers and optical switches for telecommunication, and may enable new applications spanning from high power electronic devices, energy storage devices to novel nanoporous membranes.

REFERENCES

1. K. Hata, D. N. Futaba, K. Mizuno, T. Namai, M. Yumura, S. Iijima: Science 306, 1362 (2004)

2. D. N. Futaba, K. Hata, T. Namai, T. Yamada, K. Mizuno, Y. Hayamizu, M. Yumura and S. Iijima: J. Phs. Chem.B, 110, 835(2006).
3. D. N. Futaba, K. Hata, T. Yamada, K. Mizuno, M.otoo Yumura, and S. Iijima: Phys. Rev. Lett. 95,056104 (2005).
4. T. Yamada, T. Namai, K. Hata, D. N. Futaba, K. Mizuno, J. Fan, M. Yudasaka, M. Yumura, S. Iijima: Nature Nanotechnology 1, 131,(2006).
5. T. Hiraoka, T. Yamada, K. Hata, D. N. Futaba, H. Kurachi, S. Uemura, M. Yumura, S. Iijima: J. Am. Chem. Soc. 128, 13338 (2006).
6. D. N. Futaba, K. Hata, T. Yamada, T. Hiraoka, Y. Hayamizu, Y. Kakudate, O. Tanaike, H. Hatori, M. Yumura and S. Iijima: (in print in Nature Material 10.1038/nmat1782).